SUPPLEMENTAL DATA

Supplemental Figure 1

G-insertion identified among previously reported variations in *FMR1*

(A) Summary of previously unreported intragenic variations in *FMR1* in 7 males. The subject of the study is indicated in bold.

(B) Guanine insertion in exon 15 [1457insG] of FMR1 identified in the subject of the study.

Supplemental Figure 2

Patient C-terminus encodes a functional nuclear localization signal (NLS).

(A) HEK293 cells transfected with vectors encoding mCherry-tagged wild type profilin *(mCherry-Profilin*) or mCherry-tagged profilin fused with the patient NLS sequence (*mCherry-Profilin*$^{+NLS}$). Wild type profilin is cytoplasmic, however, when fused to the NLS peptide, aggregates in nuclear inclusions.

Western blot analysis depicting expression levels of the different FMRP variants studied in the cell culture. A GFP-antibody was used on whole cell lysates of HEK293 cells transfected with the different GFP-FMR1 fusion constructs. Anti-actin was used for validation of protein load. Expression levels do not correlate with localization phenotypes. Scale bar represents 10μm.

Supplemental Figure 3

Sequence alignment of FMR/FXR protein family

(A) Amino acid alignment of human FMRP, FXR1P, FXR2P, mouse FMRP and fly FMRP. N-terminus is highly conserved while the C-terminus is more variable. The protein sequences (accession numbers # AAB28395.2, AAC50155.1, NP004851.2, NP032057.2, AAF54493.2) were aligned with the multiple sequence alignment (MUSCLE) function of MEGA6 (Tamura et al. 2013) using the default parameters and the alignment was corrected manually.

The black asterisk indicates the corresponding location of the patient mutation. The red asterisk shows the location of the C-terminus truncation engineered in the *dfmr1* variants (i.e. *dfmr1*$^{\Delta Ct}$ and *dfmr1*$^{\Delta Ct\ +NLS}$).

Supplemental Figure 4

Protein levels of *dfmr1* variants tested

(A) A pan-neuronal driver (Elav-Gal4) was used to express the different *dfmr1* variants and protein expression levels were determined via western blot analysis of adult fly brain protein extracts. Anti-Gapdh was used for validation of protein load. The graph shows changes in expression level of the different Dfmrp isoforms relative to wild type. Expression levels do not correlate with axonal phenotypes. For example, the relative expression levels of $Dfmrp^{wt+NLS}$ and Dfmrp $^{\Delta Ct+NLS}$ are comparable, yet unlike $Dfmrp^{wt+NLS}$, Dfmrp $^{\Delta Ct+NLS}$ fails to cause axonal collapse. Similarly, novel axonal misguidance phenotypes are only observed with Dfmrp $^{\Delta Ct+NLS}$ expression.

Supplemental Figure 5

Increasing Dfmrp expression in LNv neurons does not cause changes in axonal and subcellular localization phenotypes.

(A) Further increasing expression of wild type Dfmrp in LNv neurons does not alter axonal collapse phenotypes. As observed for one copy of UAS-dfmr1, two copies of UAS-dfmr1 cause strong axonal collapse. However, no misguidance phenotypes are observed (n=20). Scale bar represents 10μm.

(B) Independent of expression levels, Dfmrp is predominantly cytoplasmic in LNv neurons. Scale bar represents 5μm.

Supplemental Fig 1

A

Genomic Position	Type	Annotation
9896	A>G	intronic
10056	T>C	intronic
16812	G>A	Coding, silent
24421	C>T	intronic
32758	G>T	intronic
32825	delC	intronic
33020	**insG**	**coding, frameshift**

B

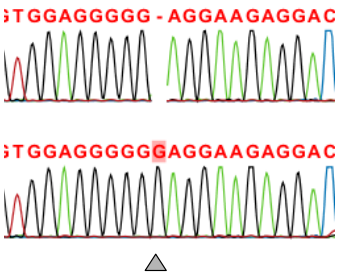

Supplemental Fig 2

A

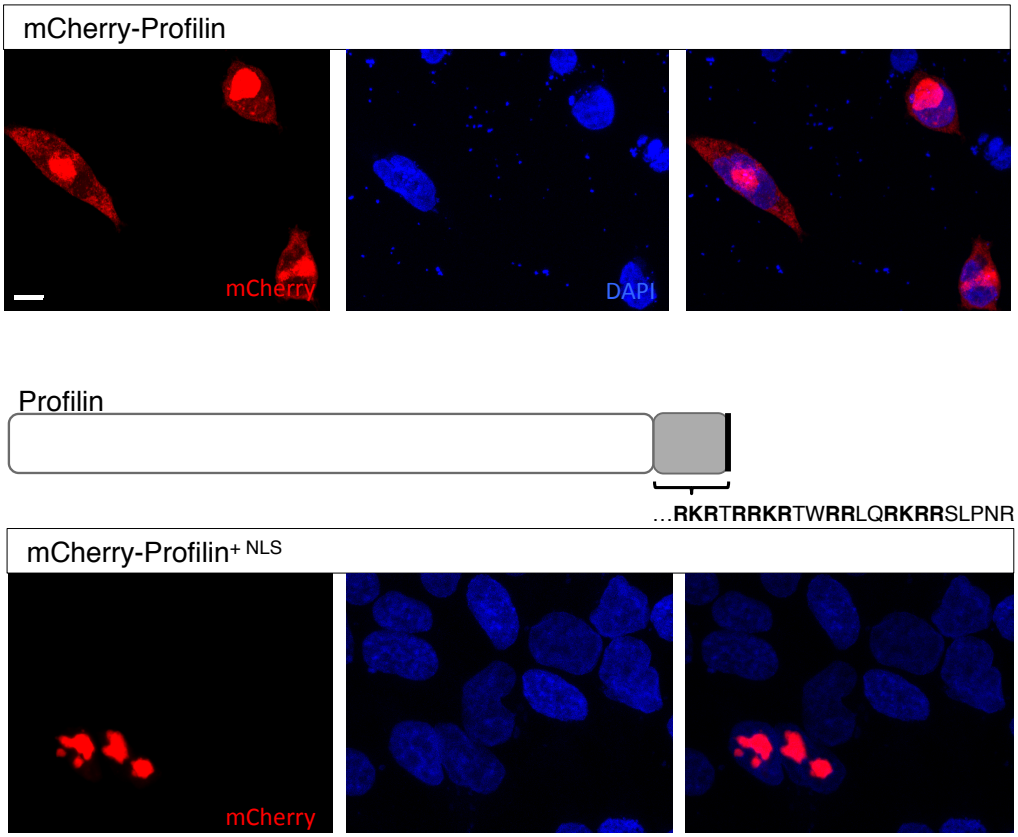

B

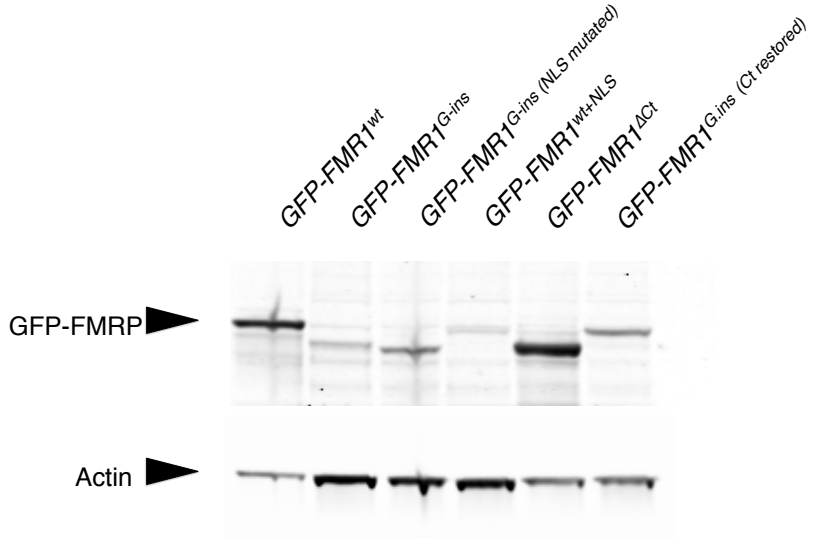

Supplemental Fig 2

A

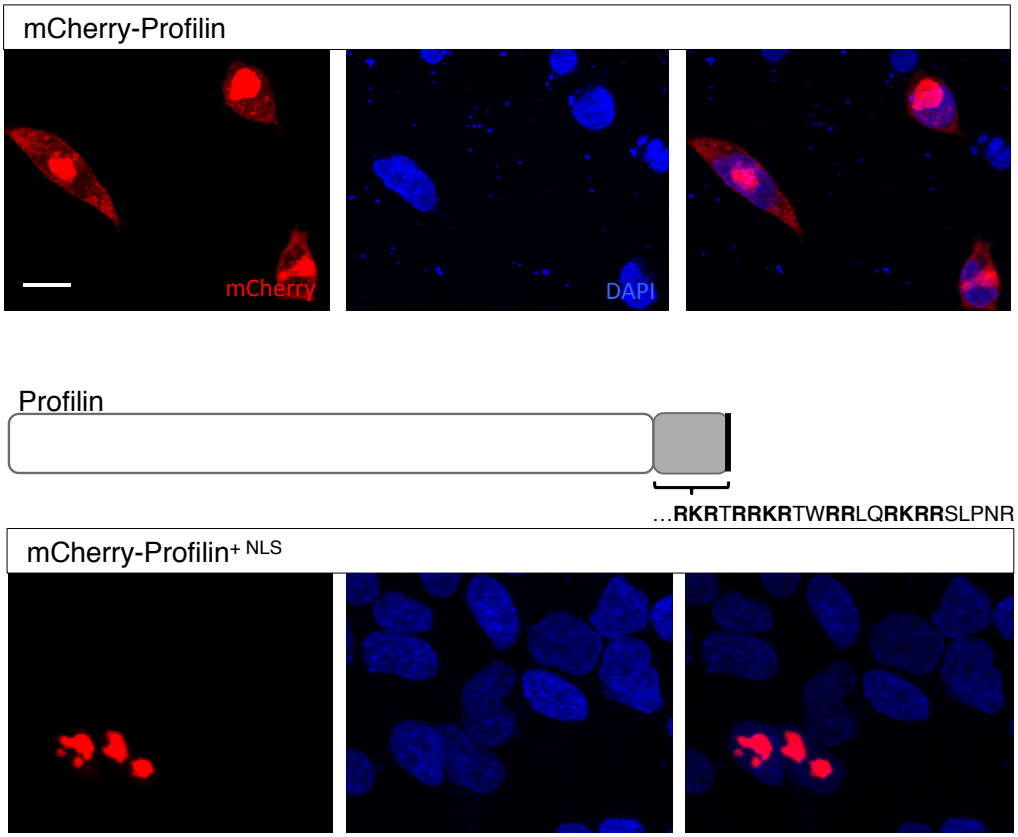

B

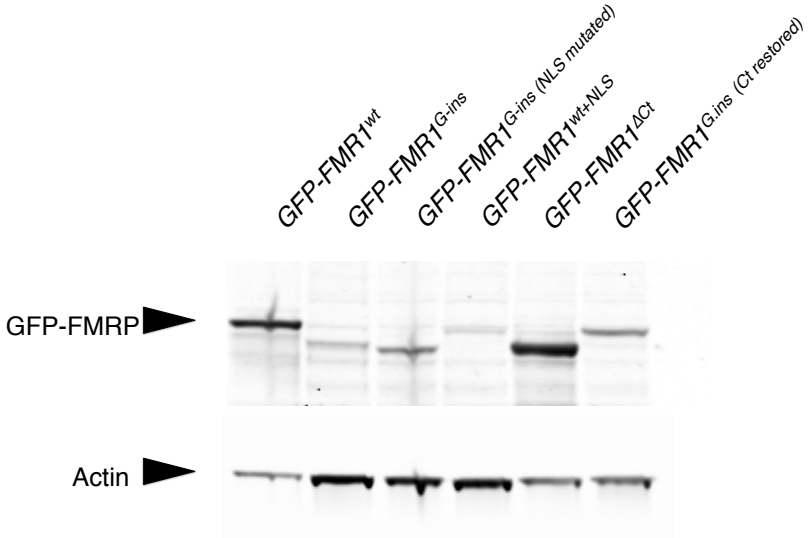

Supplemental Fig 3

A

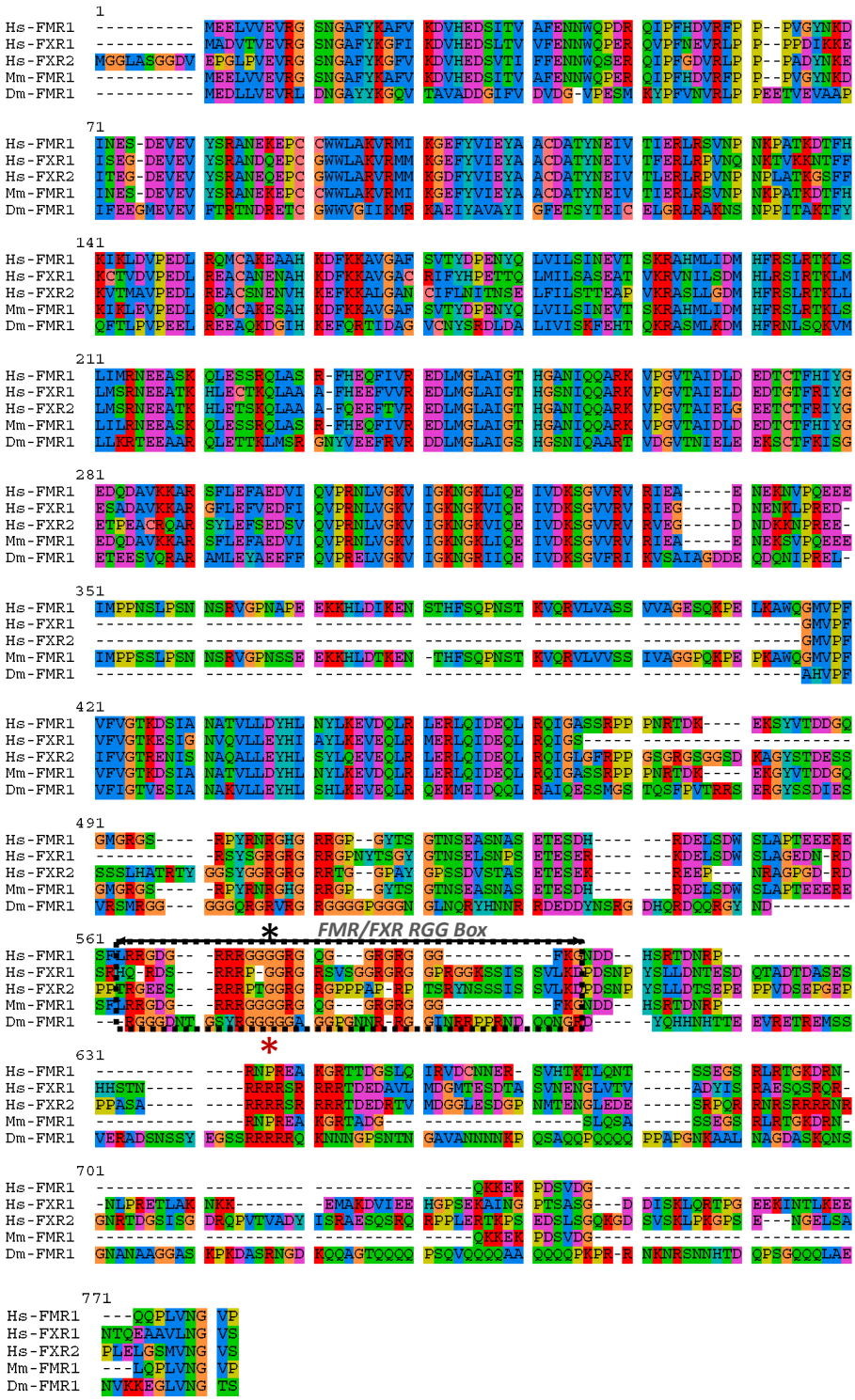

Supplemental Fig 4

A

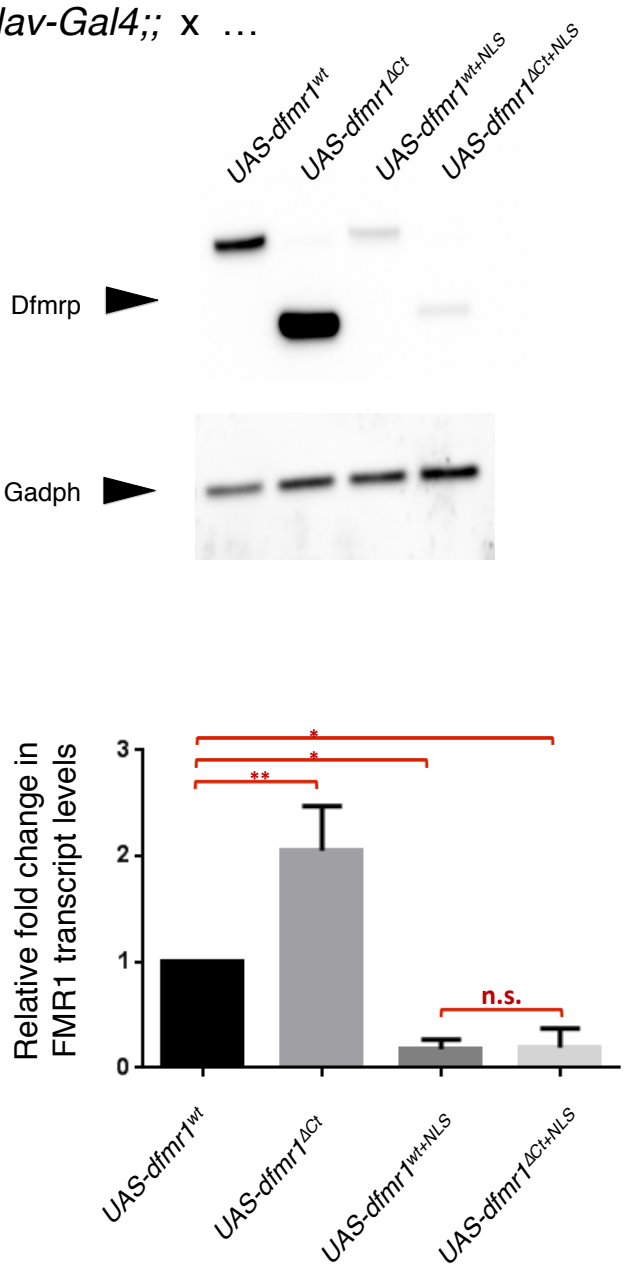

Supplemental Fig 5

A

Pdf-Gal4, UAS-CD8-GFP x …

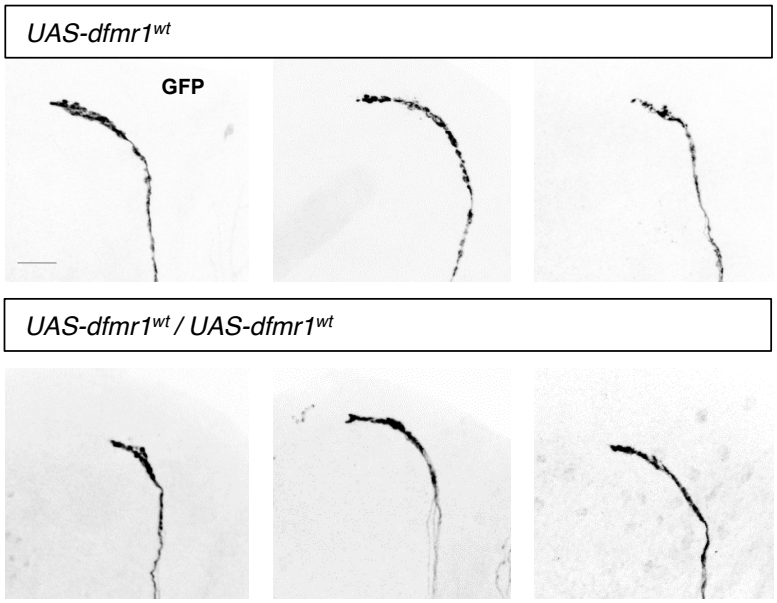

B

Pdf-Gal4, UAS-CD8-GFP x …